

## Automatic discontinuity extraction for 3-D seismic images

Jun Ji<sup>1</sup>

### ABSTRACT

A goal of seismic processing is to verify the spatial characteristics of the subsurface. Achieving this goal often requires human analysis to interpret geologically meaningful discontinuities from the seismic image. This interpretation is a challenging task even for an experienced interpreter if the image is 3D. This paper introduces an automatic method to extract seismic event discontinuities from a 3D seismic image. The proposed method consists of three steps. The first step is to evaluate the coherency of seismic events from the seismic image. The second step is to express the regions where discontinuities may exist in a binary image form. The third step is to locate the discontinuity surfaces by thinning the region found in the second step.

### INTRODUCTION

In the oil and gas industry, subsurface imaging with the reflection seismic method has been performed for many decades and has been accepted as a successful approach. The procedure of subsurface imaging from raw seismic data consists of many complicated sub-processes and is often organized differently according to its various purposes. In many cases, however, human interpretation of event discontinuity that indicates faults, unconformities, and buried channels is required during processing, or at the end of the procedure. Such interpretations are usually accomplished by an experienced interpreter who has in-depth knowledge of geology. Even for an experienced expert, the interpretation task is challenging if the image is a 3D volume.

In order to help with such tasks, a process called “coherency evaluation” has been developed (Bahorich and Farmer, 1995; Marfurt et al., 1998). The coherency evaluation calculates continuity of seismic events from a 3D seismic image cube and produces a so-called “coherency cube” that shows the distribution of the event continuity in a 3D volume. The output of coherency evaluation processing helps the interpreters to locate geologically meaningful discontinuities more easily. However, interpreting and mapping 3D discontinuity surfaces by hand is still a challenging job because of the difficulty in visualizing a 3D image and the complexity of surfaces in a 3D sense.

As a supplementary tool for mapping discontinuities, I introduce an automatic discontinuity extraction method. The proposed method starts with a coherency evaluation for a 3D seismic image and produces a discontinuity map that locates the event’s discontinuities in the

---

<sup>1</sup>email: jun@sep.stanford.edu

form of arbitrarily shaped 3D surfaces. The output of the proposed method could be a good starting point for an interpreter to narrow down the various discontinuities into more meaningful geological features such as faults, unconformities, and buried channels.

In the following section I will shortly review the coherency evaluation method to clarify the meaning of a discontinuity in a seismic image. The subsequent two sections are devoted to explaining the following procedures. In each step, the algorithm is explained and also demonstrated with a real seismic image. The testing image used is from the Boonsville natural gas field located in north-central Texas and was acquired by the DOE and the Gas Research Institute as part of a secondary gas recovery technique development. According to Hardage (Hardage, 1996), the Boonsville seismic image is a full-fold time migrated section with  $110m \times 110m$  in bin size and covers  $5.5km^2$  area. The data consists of 97 lines along the crossline and each line has 113 traces. Figure 1 shows three plane sections of the image volume which are orthogonal to each other.

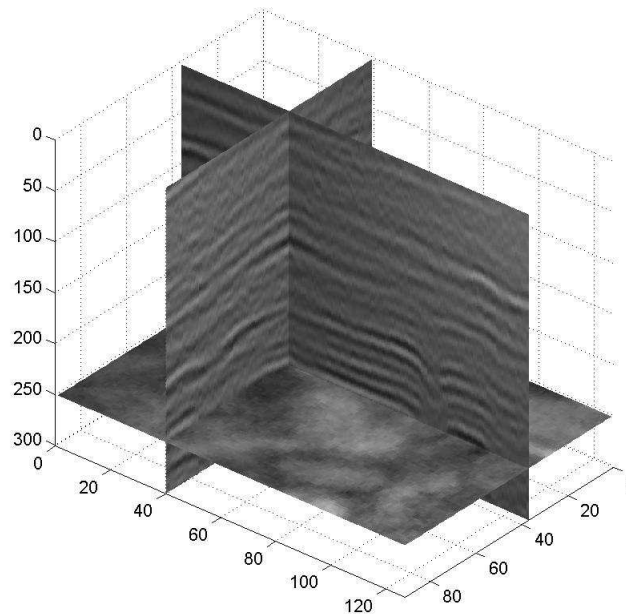


Figure 1: Three selected sections of Boonsville 3D seismic image (time slice at  $t = 250ms$ , the 37th crossline section, and the 40th inline section.) [jun1-seis](#) [NR]

## COHERENCY EVALUATION FOR SEISMIC EVENTS

Coherency evaluation has been widely used to estimate the continuity of seismic events for a given seismic image. There are several approaches, including the cross-correlation method (Bahorich and Farmer, 1995) and the semblance method (Marfurt et al., 1998). In this paper, I used the semblance method which is an improvement on the the early cross-correlation

method. The following is a short review of the method. First of all, as you can see in Figure 2, I define an elliptic plane that contains  $J$  traces around the trace where the coherency is calculated. Then the semblance  $s$  at the center of the ellipse for every dip direction is defined as follows:

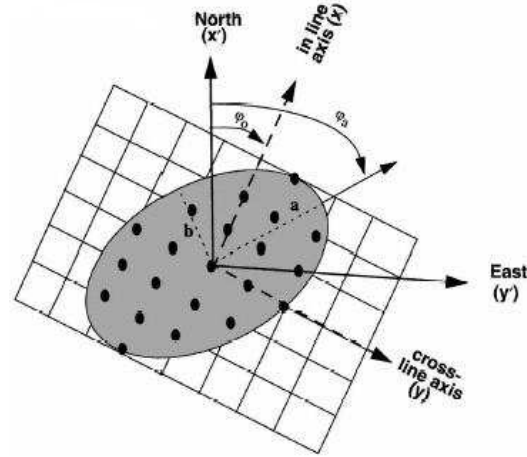
$$s(t, x, y, p, q) = \frac{\sum_{k=-K}^K \left\{ \left[ \sum_{j=1}^J u(t_{j,k}, x_j, y_j) \right]^2 + \left[ \sum_{j=1}^J u^H(t_{j,k}, x_j, y_j) \right]^2 \right\}}{J \sum_{k=-K}^K \sum_{j=1}^J \left\{ \left[ u(t_{j,k}, x_j, y_j) \right]^2 + \left[ u^H(t_{j,k}, x_j, y_j) \right]^2 \right\}} \quad (1)$$

with

$$t_{j,k} = t + k\Delta t - px_j - qy_j$$

where  $u$  is the image data, the superscript  $H$  represent the Hilbert transform,  $p$  and  $q$  are the dips of elliptic plane along  $x$  and  $y$  axes direction, respectively. In order to suppress a possible high coherency value around the zero-crossing location, the average semblance is calculated along a time window that ranges from upper  $K$  to lower  $K$ . As evident in equation (1), the

Figure 2: Elliptic analysis window centered about an analysis point including  $J$  traces. jun1-ellipse [NR]



coherency analysis requires average semblances for various dips (Figure 3). The method of choosing the dips is important not only for the computational cost, but also to obtain an even distribution of dips. I used a “Chinese checker” tessellation (Marfurt et al., 1998) to find a finite number of discrete angle combinations. Then the coherency value at each location was determined by choosing a maximum value among the semblance values for various dips as follows:

$$coh(t, x, y) = \text{Max}_{p,q} s(t, x, y, p, q). \quad (2)$$

This coherency evaluation is performed for the Boonsville image and the result is shown in Figure 4. In Figure 4, the coherency values are shown in grey scale so that the dark represent low coherency and the bright represent high coherency. A comparison of Figure 4 to Figure 1, shows that the coherency cube more clearly reveals the discontinuities in the seismic image. It shows not only the discontinuities that were obvious, but also the ones that are hard to recognize in the seismic image.

Figure 3: Calculation of coherency over an elliptical analysis window with apparent dips (Marfurt et al., 1998). `jun1-dip` [NR]

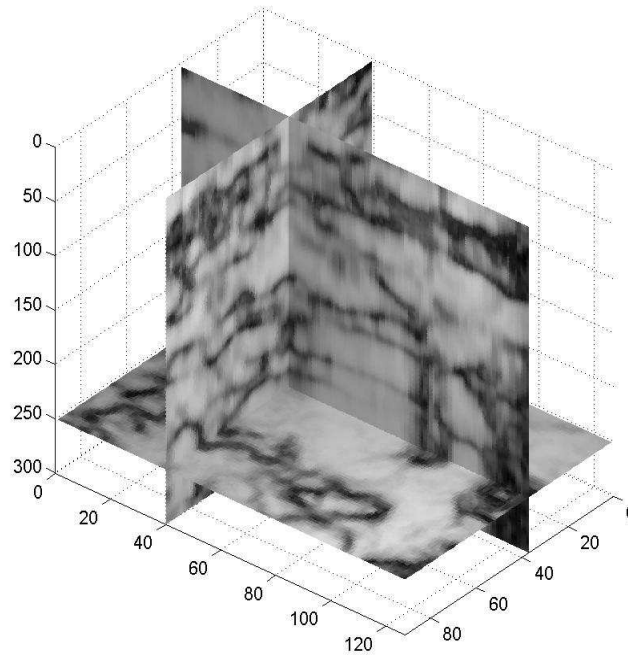
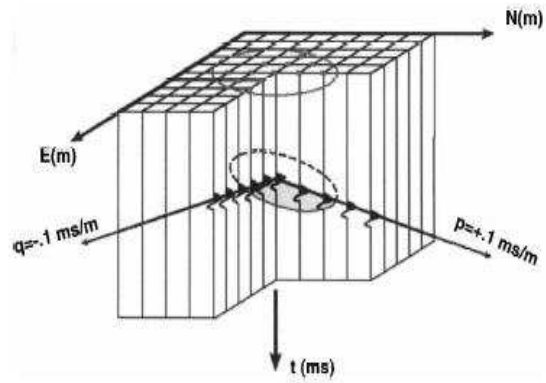


Figure 4: Selected sections of coherency cube of the Boonsville image. `jun1-coh` [NR]

## LOCATING REGIONS FOR POTENTIAL DISCONTINUITY LOCATIONS

The coherency evaluation explained in the previous section will produce a coherency cube for a 3D seismic image. In the coherency cube, the discontinuity information is expressed as a distribution of the event continuity with numerical values ranging from 1 to 0 corresponding to the semblance of events at each location. A conventional interpretation process takes another step to map the discontinuity surfaces with the help of various visualization tools.

It is obvious that the discontinuity surfaces will be located somewhere in the region where the coherency value is lower than its neighbor. The shape of the discontinuity surface will be similar to the shape of the region that has lower coherency values than others. Therefore, a rough 3D shape of the discontinuity surfaces can be obtained in a binary image form obtained by thresholding the coherency cube as follows:

$$B(t, x, y) = \begin{cases} 0 & \text{if } coh(t, x, z) \leq coh_{th} \\ 1 & \text{otherwise} \end{cases} \quad (3)$$

where the thresholding value,  $coh_{th}$ , is determined empirically with a trial and error approach. The image needs to be histogram-equalized before thresholding, which requires the image to be quantized. I quantized the coherency value by rounding it to the nearest hundredth value, then applied histogram equalization to make sure each coherency value is distributed evenly so that the thresholding value change effects for the binary image shape appropriately. Figures 5 and 6 show the histogram of quantized coherency values and its result after histogram equalization, respectively. The effect of the quantization and the equalization on the image can be seen in Figures 7 and 8. By increasing the contrast, the unclear low coherency region in Figure 7 becomes clear in Figure 8.

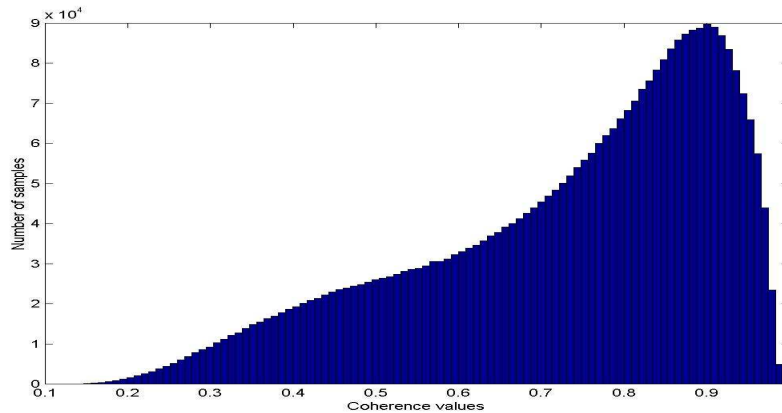


Figure 5: Histogram of the quantized coherency cube. jun1-histogram [NR]

The effects on the binary image shape with respect to different thresholding values are shown in Figures 9 through 11. Figure 9, 10 and 11 are images obtained by thresholding Figure 8 with 0.2, 0.3, and 0.4, respectively. From those figures, we can see that increasing the thresholding value makes the binary image shape get thicker, as expected.

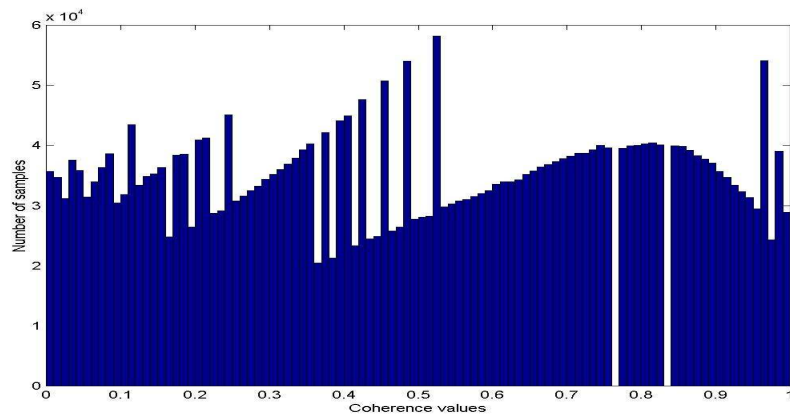


Figure 6: Histogram of the quantized coherency cube after histogram equalization.

`jun1-histogrameq` [NR]

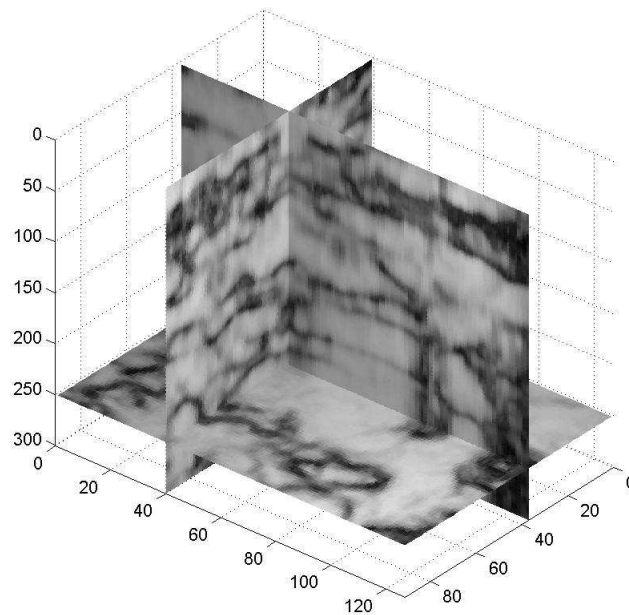


Figure 7: The coherency cube after quantization applied with 0.01 quantization level.

`jun1-coh-quantize` [NR]

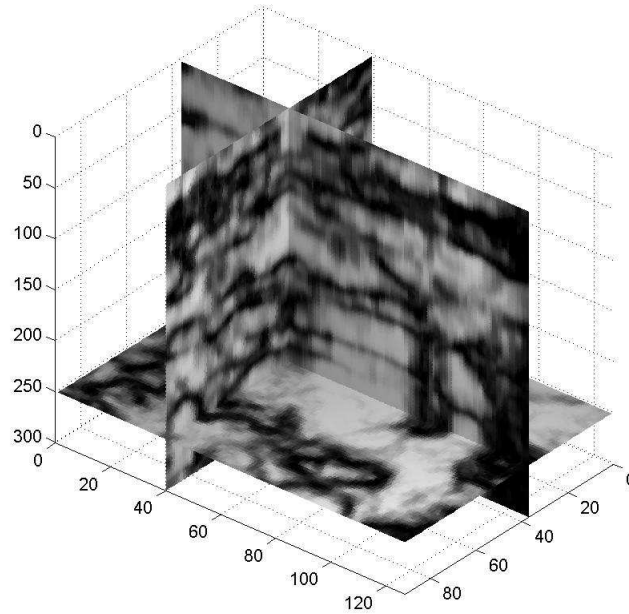


Figure 8: The coherency cube after the histogram equalization applied. `jun1-coh-heq` [NR]

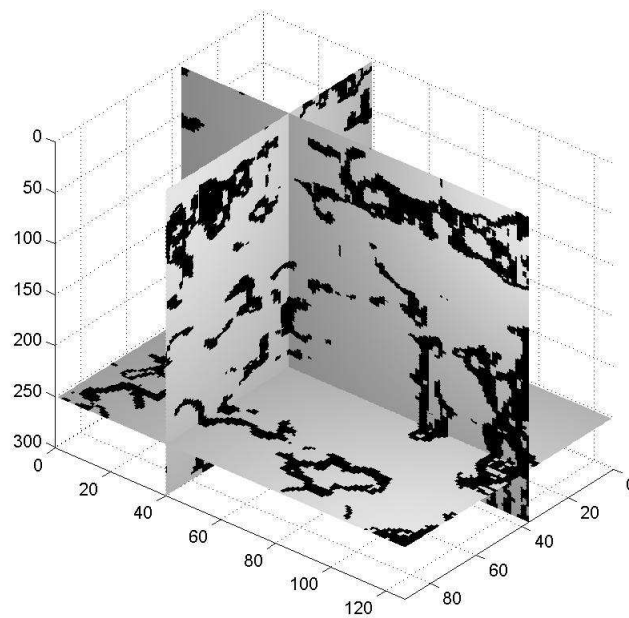


Figure 9: Binary image obtained by selecting points whose values are less than 0.2 from the histogram equalized coherency cube. `jun1-binary20` [NR]

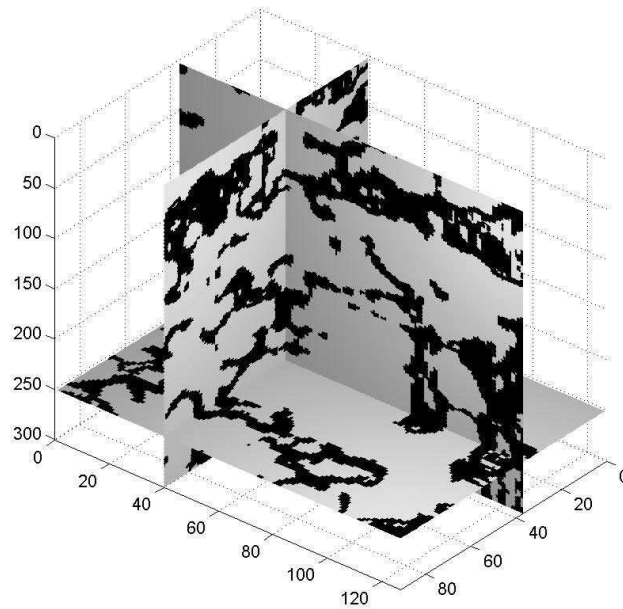


Figure 10: Binary image obtained by selecting points whose values are less than 0.3 from the histogram equalized coherency cube. `jun1-binary-30` [NR]

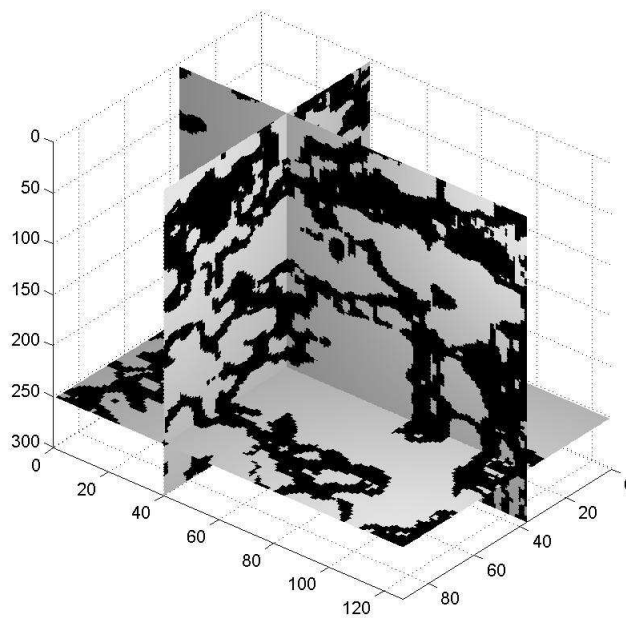


Figure 11: Binary image obtained by selecting points whose values are less than 0.4 from the histogram equalized coherency cube. `jun1-binary-40` [NR]



## DISCONTINUITY SURFACE EXTRACTION

The binary image obtained in the previous section represents the shape of the region where the discontinuity surfaces may exist. Therefore, the discontinuity location could be found by thinning the 3D binary image. There are various thinning algorithms developed in the image processing field and they have been used for various applications in topological analysis. I used a 2D thinning algorithm and adapted it into 3D image skeletonization.

The conventional 2D thinning algorithm can be explained as follows: for a given pixel location whose value is 1, its value will be changed to 0 if the neighboring pixels have values like one of the patterns shown in equation (4). This operation continues until no pixels change. It will leave thin lines a pixel in width. The structure elements used in 2D thinning are given as follows:

$$\mathbf{L}_1 = \begin{bmatrix} 0 & 0 & 0 \\ * & 1 & * \\ 1 & 1 & 1 \end{bmatrix}, \quad \mathbf{L}_2 = \begin{bmatrix} * & 0 & 0 \\ 1 & 1 & 0 \\ * & 1 & * \end{bmatrix}, \dots \quad (4)$$

where the central location “1” corresponds to the pixel for operation and “\*” corresponds to unused pixels. The rest of the 6 elements can be found by rotating the above element appropriately (Sonka et al., 1999). Direct extending this 2D algorithm into a 3D algorithm, will result in a 3D thinning algorithm that produces 3D lines (Ma and Sonka, 1996). Such line searching does not meet our goal of finding 3D surfaces by squeezing a 3D region. Therefore, I iteratively applied the 2D thinning algorithms for each orthogonal direction, resulting in the desired 3D thinning algorithm.

First, the 2D thinning algorithm is applied once for each  $(x, y)$ ,  $(y, z)$ , and  $(x, z)$  plane separately, and the pixel is considered to be removed only if the removal happens in at least two of the three planes. The thinning continues until no pixels change. Finally, this results in 3D surfaces with a width of one pixel, representing the locations of discontinuities. This process can be summarized in a pseudo code as follows:

```
old_data(x, y, z) = binary_data(x, y, z)
condition = 1
do while (condition .eq. 1)
{
temp1(x, y, z) = 2D thinning along every (x, y) plane on old_data(x, y, z)
temp2(x, y, z) = 2D thinning along every (y, z) plane on old_data(x, y, z)
temp3(x, y, z) = 2D thinning along every (x, z) plane on old_data(x, y, z)
new_data = [(temp1.and.temp2).or.(temp2.and.temp3).or.(temp1.and.temp3)]
if(new_data .eq. old_data) { condition = 0 }
else { old_data(x, y, z) = new_data(x, y, z) }
}
```

The above 3D thinning algorithm is applied to the three differently thresholded images shown in Figure 9, Figure 10, and Figure 11. The results are shown at Figure 12, Figure 13, and Figure 14, respectively. These figures show that as the thresholding value increases, more

detailed shapes of the discontinuities can be found without affecting the major structure of the discontinuity surfaces. This reveals the robustness of the method in choosing the threshold values. By overlapping the discontinuity map onto the original coherency cube, we can see that the locations of discontinuities are accurately positioned, as expected (Figure 15).

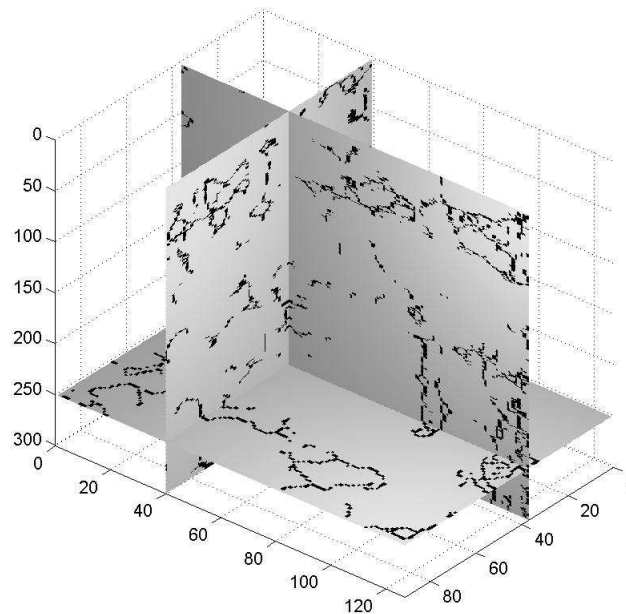


Figure 12: Discontinuity surfaces found by thinning the binary image with thresholding value of 0.2. `jun1-thin20` [NR]

## CONCLUSIONS

I describe an automatic algorithm for discontinuity extraction from a 3D seismic image cube. The proposed algorithm consists of three steps. The first step is the coherency computation which results in a coherency cube that gives event semblance at each point. Then next step is to represent the potential discontinuity locations in binary image form. This is accomplished by thresholding the histogram-equalized coherency cube. The final step is finding location of the discontinuity by thinning the binary image obtained in the previous step. For thinning in the 3D sense, a 2D thinning algorithm is consecutively applied to produce an arbitrary shaped 3D surface.

Testing the algorithm on a real seismic image demonstrated that it can successfully find discontinuity surfaces. The extracted discontinuity surfaces could be interpreted as fault, unconformity, or buried channel. However, in order to make the proposed algorithm a more useful tool that produces geologically meaningful surfaces, further research needs to be followed. Two areas of research are: (1) The development of topological relationships between

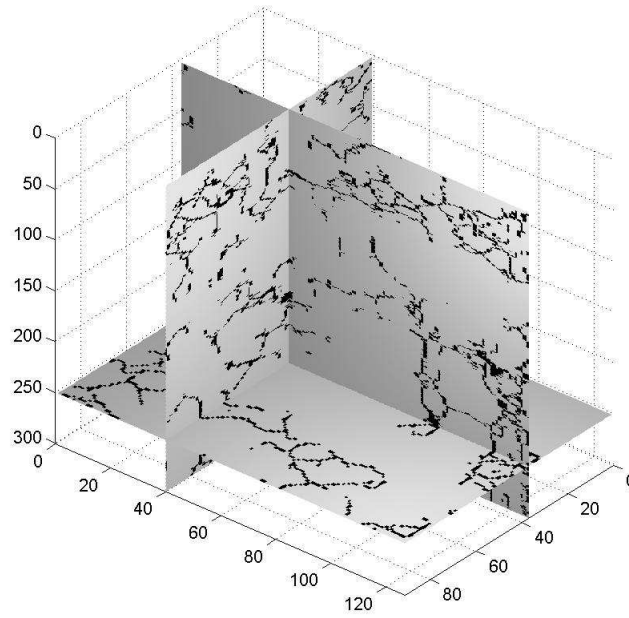


Figure 13: Discontinuity surfaces found by thinning the binary image with thresholding value of 0.3. `jun1-thin30` [NR]

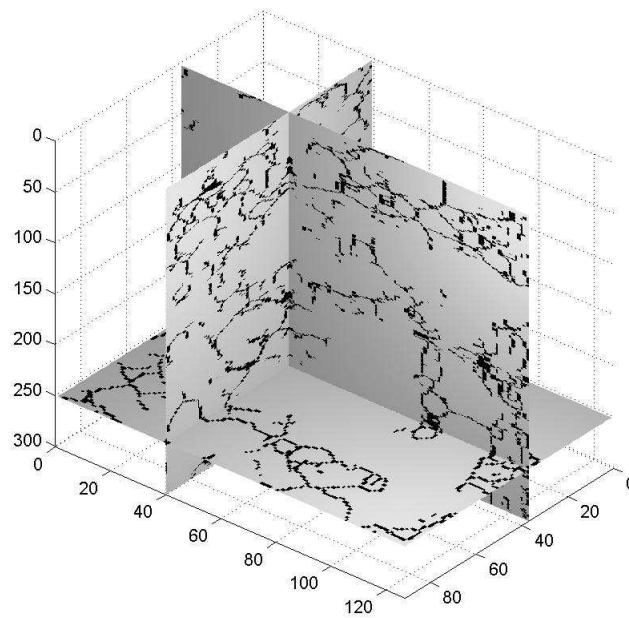


Figure 14: Discontinuity surfaces found by thinning the binary image with thresholding value of 0.4. `jun1-thin40` [NR]

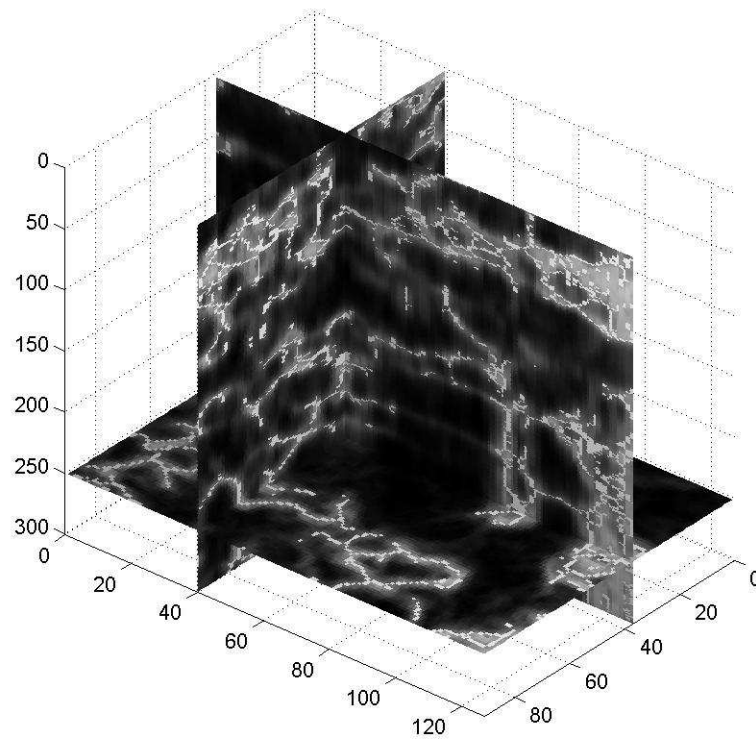


Figure 15: Discontinuities with thresholding value of 0.3 are overlapped with coherency cube to examine the accuracy of the location. To visualize the location of the discontinuities, low values in the coherency cube are expressed in bright grey and high values are expressed in dark grey. `jun1-thincoh30` [NR]

surfaces to determine whether they are connected or not. and (2) The inclusion of smoothness criteria, as geology may often dictate that some discontinuity surfaces are expected to be smooth.

### REFERENCES

- Bahorich, M., and Farmer, S., 1995, 3-D seismic discontinuity for faults and stratigraphic features: The coherence cube: *The Leading Edge*, **14**, no. 10, 1053–1058.
- Hardage, B. A., 1996, Boonsville 3-d data set: *The Leading Edge*, **15**, no. 7, 835–837.
- Ma, M. C., and Sonka, M., 1996, A fully parallel 3d thinning algorithm and its application: *Computer vision and image understanding*, **64**, no. 03, 420–433.
- Marfurt, K. J., Kirlin, R. L., Farmer, S. L., and Bahorich, M. S., 1998, 3-D seismic attributes using a semblance-based coherency algorithm: *Geophysics*, **63**, no. 04, 1150–1165.
- Sonka, M., Hlavac, V., and Boyle, R., 1999, *Image processing, analysis, and machine vision*: 2nd-edition: PWS Publishing.

